REVISTA DE METALURGIA, 47 (6)
NOVIEMBRE-DICIEMBRE, 497-506, 2011
ISSN: 0034-8570
eISSN: 1988-4222
doi: 10.3989/revmetalm.1146

Pitting corrosion in austenitic stainless steel water tanks of hotel trains(·)

D.A. Moreno*, A. M. García*, C. Ranninger* and B. Molina**

Abstract

The water storage tanks of hotel trains suffered pitting corrosion. To identify the cause, the tanks were subjected to a detailed metallographic study and the chemical composition of the austenitic stainless steels used in their construction was determined. Both the tank water and the corrosion products were further examined by physicochemical and microbiological testing. Corrosion was shown to be related to an incompatibility between the chloride content of the water and the base and filler metals of the tanks. These findings formed the basis of recommendations aimed at the prevention and control of corrosion in such tanks.

Keywords: Pitting corrosion; Austenitic stainless steel; Welding; Water tank; Hotel train.

Corrosión por picaduras en depósitos de agua de acero inoxidable austenítico en trenes hotel

Resumen

Se han detectado problemas de corrosión por picaduras en los depósitos de agua de trenes hotel. Para identificar las causas se llevó a cabo un detallado estudio metalográfico así como de la composición química de los aceros inoxidables austeníticos utilizados en su construcción. También se realizaron estudios fisicoquímicos y microbiológicos de los productos de corrosión. Se ha encontrado que los problemas de corrosión están relacionados con la incompatibilidad entre el contenido en cloruros del agua y los metales base y de aporte de la soldadura de los tanques. En base a estos hallazgos se proponen una serie de recomendaciones encaminadas a la prevención y control de la corrosión de dichos depósitos.

Palabras clave: Corrosión por picaduras; Acero inoxidable austenítico; Soldadura; Depósito de agua; Tren hotel.

1. INTRODUCTION

In 2007 and 2008, Patentes Talgo built nine hotel trains for long-distance travel in Spain. After a few months of service, pitting corrosion could be seen in the 250 and 455-L water tanks used to supply the trains' toilets and showers. Once the corrosion was detected, the tank was either repaired with a resin, using a procedure known as "cold welding," or, in extremes cases, replaced with a new one. However, within a few months time the new tanks had similar corrosion problems. A study was therefore carried out to determine the cause of the corrosion and to formulate recommendations for its prevention and control.

The water tanks were manufactured using two types of austenitic stainless steel as the base metal, AISI 316Ti, in 2007, and, beginning in 2008, the less expensive (by 25 %) AISI 321. In both cases, ER347 was used as the filler metal. Table I lists the water tanks that had corrosion problems. In less than one year, pitting corrosion affected 46 of the 95 water tanks made with AISI 321, i.e., half the tanks in service. By contrast, among the 64 tanks made with AISI 316Ti, only one became corroded, after 2 years in service. Therefore, the present study focused on the AISI 321 titanium-stabilized tanks currently in use. The initial assumption of the tank's manufacturer and the end user was that either there was an error in the tank-manufacturing process or sulfate-reducing bacteria

(·) Trabajo recibido el día 06 de septiembre de 2011 y aceptado en su forma final el día 07 de octubre de 2011.
* Universidad Politécnica de Madrid, Departamento de Ingeniería y Ciencia de los Materiales, Escuela Técnica Superior de Ingenieros Industriales, José Gutiérrez Abascal, 2 - E-28006 Madrid, SPAIN. Corresponding author: D.A. Moreno, Tel.: +34 913 363 164. Fax: +34 913 363 007. *E-mail address*: diego.moreno@upm.es.
** Patentes Talgo SL, Oficina Técnica, Paseo del Tren Talgo 2 - E-28290 Las Matas, Madrid, SPAIN.

Table I. Corrosion problems detected in austenitic stainless steel water tanks from Patentes Talgo's luxury hotel trains (from 2007 to 2009)

Tabla I. Problemas de corrosión detectados en los depósitos de agua de acero inoxidable austenítico de trenes hotel de lujo de Patentes Talgo (de 2007 a 2009)

Hotel Train Code	**7C1**	**7C2**	**7C3**	**7C4**	**7C5**	**7C6**	**7C7**	**7C8**	**7C9**	
Manufacturing Date	**2007**	**2007**	**2007**	**2007**	**2008**	**2008**	**2008**	**2008**	**2008**	**TOTAL**
250-Liter Water Tanks										
Manufactured with 316Ti SS	12	20	20	12						64
Corroded after 2 years	0	0	0	1						1
Manufactured with 321 SS					19	19	19	19	19	95
Corroded after 1 year					8	9	7	4	18	46
455-Liter Water Tanks										
Manufactured with 321 SS	6	6	6	6	6	6	6	6	6	54
Corroded after 1 and 2 years	3	0	0	6	2	0	0	0	3	14

(SRB) were present in the water stored in the tanks. It is known that stainless steel is not immune to pitting corrosion when in the presence of the corrosive action of microorganisms and mainly SRB[1 and 2]. Among the types of stainless steel affected by microbiologically influenced corrosion (MIC), the vulnerability of austenitic stainless steel of the 300 series, both normal grades (e.g., AISI 304 and AISI 316) and low-carbon grades (e.g., 304L and 316L)[1 and 2], and of titanium stabilized grades (e.g., AISI 321)[3] to MIC is well documented. In addition, MIC often occurs preferentially in the weld metal of austenitic stainless steel, initiating at the weld fusion line and progressing into the weld metal[4 and 5]. The degree of bacterial attack is a strong function of the material's pitting resistance and is thus more common in alloys without Mo than in those with Mo[6].

2. MATERIALS AND METHODS

2.1. Visual inspection

Water tanks removed from hotel train 7C9 due to pitting corrosion problems were visually inspected at the Patentes Talgo plant in Rivabellosa (Álava, Spain). The cylindrical tanks have torispherical heads and in service are placed in a horizontal position. One 250-L tank, removed from a shower car in the last train built in 2008, was chosen for the study. The tanks showed signs of pitting corrosion only a few months after it had been put into service as well as evidence of several subsequent repairs (Fig. 1). All the repairs involved the tank's lower zone, where most of the nozzles were located. The tank's upper zone was not corroded (Fig. 2).

The 250-L tank was 3.00 mm thick and had the following welds:

— Two circumferential head to shell weld seams and one circumferential shell to shell- plate weld seam.

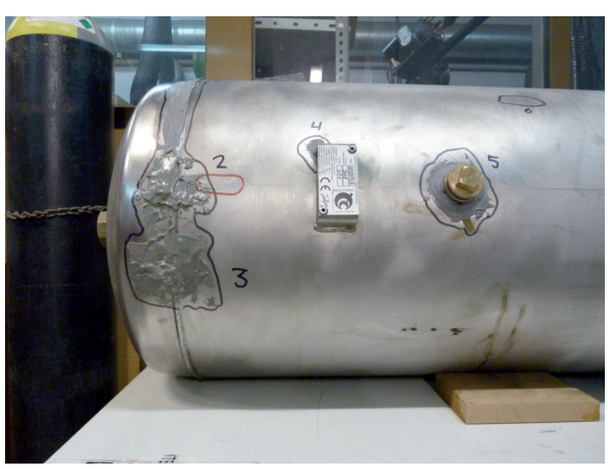

Figure 1. Aspect of the 250-L water tank around the lower zone (head 1). The repairs, made with resin, are seen.

Figura 1. Aspecto del depósito de agua de 250 litros en su zona inferior (cabeza 1). Pueden observarse las reparaciones realizadas con resina.

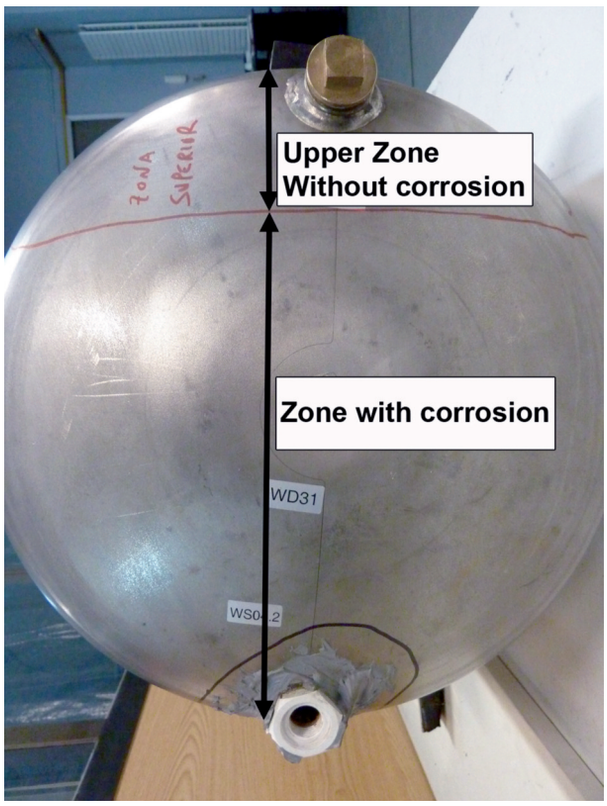

Figure 2. View of head 2 of the 250-L water tank, with corrosion and non-corrosion zones indicated.

Figura 2. Vista de la cabeza 2 del depósito de agua de 250 litros, indicándose las zonas de corrosión y sin corrosión.

— Two longitudinal weld seams at the two shell plates, one at 2/3 of the distance between the two heads and the other at 1/3 of that distance. The two weld seams were 180° opposite to each other.
— Several welds in the nozzles, in the anchors supporting the tank, and in the shell plate and internal stiffeners.

Corrosion was limited to the area between the base metal and the weld metal. Of the 12 points of corrosion detected, five were located in the nozzles, five at the circumferential seams, and two at the longitudinal weld seams. The circumferential seams of the tank's head to shell welds were the most extensively affected and thus probably the first to suffer corrosion.

Visual inspection revealed pitting in one of the longitudinal weld seams that had not been repaired. This pitting site was denoted F - 41 and was chosen for the corrosion study, as it had not been manipulated. It was also of interest to study the corrosion of nozzle F - 11, whose AISI 316 nipple had been welded to AISI 321 with ER347.

2.2. Characterization of austenitic stainless steel

The quality of the stainless steel used in manufacturing the eventually corroded water tanks was evaluated by chemical testing of the base metal and the weld seam. Si, Mn, P, Cr, Mo, Ni, Ti, Nb, and Cu were determined by atomic emission spectrometry (Thermo Scientific ARL 3460) on the prepared outer surface of the base metal and on the prepared weld seam after weld grinding to a flat surface. C and S were determined by high-temperature combustion (Leco CS - 125), carried out on chips of the material.

The metallographic study was first carried out using an optical microscope (Nikon Eclipse L150). Microanalytical characterization of the particles and matrix was then performed using a Hitachi S - 3000N scanning electron microscope equipped with secondary electron and back- scattering electron detectors as well as X - ray energy dispersion analysis (EDX) capability. The test specimens were subjected to electrolytic etching with a 10 % oxalic acid solution, according to the technique described in Practice A of Standard ASTM A262[7].

2.3. Corrosion analysis

Once all the repaired zones had been marked and numbered, test specimens were prepared for study. These were first observed macroscopically at a magnification of 5 - 45× (Olympus SZX12) and in some cases further examined by optical (Nikon Eclipse L150) and scanning electron microscopy. In the following, the results obtained for test specimen F - 41, which had not been repaired, and for the repaired nozzle F - 11 are presented.

The corrosion products arising from the pitting of test specimen F - 41 were analyzed by X -ray diffraction (Philips PW 1830). The presence of SRB was tested by anoxic incubation of the corrosion products in Postgate B culture medium (yeast extract, 1.0 g/l; sodium lactate in 50 % solution, 5.4 ml; $MgSO_4 \cdot 7H_2O$, 1.0 g/l; $CaSO_4$, 1.0 g/l; NH_4Cl, 1.0 g/l; KH_2PO_4, 0.5 g/l; ascorbic acid, 0.1 g/l; thioglycolic acid, 0.1 ml; $FeSO_4 \cdot 7H_2O$, 0.5 g/l; de-aeration with nitrogen 15 min, pH= 7.2 ± 0.2) at 30 °C[8].

2.4. Tank-water analysis

Two samples of water from trains 7C9 and 7C8 were collected for subsequent testing. In the latter one,

corrosion problems were also found in the water tanks. Cations were determined by ICP-OES (Perkin-Elmer 4300 DV), anions by capillary electrophoresis (Millipore Quanta 4000 CE), and carbonates and bicarbonates by volumetry. Conductivity and pH were measured as well[9].

Water samples collected in sterile containers from train 7C8 were cultured in order to determine the total number of aerobic bacteria and the presence of SRB. Total aerobic bacteria were counted in serial dilutions, with 100 µl from each dilution plated on TSA (Tryptone Soy Broth, Oxoid CM - 129) supplemented with agar (UPS) purissimum (Panreac, 15 g/l) and subsequently incubated at 30 ºC. SRB were evaluated in cultures prepared from 100 ml of water filtered through Millipore filters (pore diameter 0.22 µm; Millipore GSWP02500) and incubated in Postgate B culture medium[8] at 30 ºC under anoxic conditions.

3. RESULTS AND DISCUSSION

3.1. Characterization of austenitic Stainless Steel

The chemical composition of the base and weld metals used in building the water tanks is presented in table II. The base metal corresponds to titanium-stabilized stainless steel AISI 321 (X6CrNiTi18 - 10). The carbon content of the metal is low and is similar to that of non- stabilized austenitic stainless steel in a low carbon grade. The Cr, Ni, and Ti content complies with current standards and with the specifications of Patentes Talgo. Analysis of the weld metal identified the filler metal as niobium-stabilized stainless steel ER347 (X6CrNiNb18-10), equivalent to G 19 9 Nb Si.

The microstructure of the base metal consisted of an austenitic matrix, concordant with the properties of a titanium-stabilized stainless steel AISI 321 that had been strongly roll banded. The titanium crystals were clearly distinguished by their pink colour and in some zones were aligned with the bands (Fig. 3a)). This material, from a metallographic point of view, has a microstructure consistent with its composition.

The weld metal had a dendritic structure with titanium crystals in its matrix (Fig. 3b)).The weld-metal zone close to the base metal showed a Widmanstätten microstructure, with embedded titanium crystals coming from the base metal (Fig. 3c)) since the filler metal, identified as niobium (Nb)-stabilized stainless steel ER347, lacks titanium (Ti) in its composition (Table II). The filler metal was ER347, which contains Nb and complies with the specifications of Patentes Talgo. The Ti crystals observed in the weld pool were smaller than those of the base metal and reflected the dilution of the filler metal during the welding process.

The $\delta+\gamma$ microstructure in the weld with ER347 as filler metal indicated the use during welding of a high heat input and a low cooling rate[10].

Most of the ferrite observed in austenitic stainless steel welds containing a duplex structure can be ascribed to residual primary ferrite resulting from incomplete $\delta \rightarrow \gamma$ transformation during solidification and/or to residual ferrite after Widmanstätten austenite precipitation in primary ferrite[11]. Typically, in weld metal zones close to the base metal, there is not enough time for conversion of the original Widmanstäten structure into a more austenitic structure.

The metallographic study was completed with a detailed scanning electron microscopy analysis using X - ray dispersive energy. This was accomplished by a 3,500 - 5,000× magnification of the diverse phases observed in the microstructures. The weld metal thus observed showed an austenitic matrix containing islands of delta ferrite and Nb inclusions (Fig. 4).

Table III presents comparative data from the SEM-EDX analysis and includes the different phases determined in the base metal and in the weld metal.

Table II. Chemical composition of the base and weld metals of the 250-L tank under study (% in weight)

Tabla II. Composición química de los metales base y del baño de fusión del depósito de 250 litros en estudio (% en peso)

Material	C	Si	Mn	P	S	Cr	Mo	Ni	Ti	Nb	Cu	Fe
Base Metal	0.026	0.59	1.68	0.027	0.006	17.3	0.24	9.1	0.35	0.00	0.43	Bal.
Weld Metal	0.056	0.51	1.53	0.025	0.010	18.0	0.20	9.2	0.20	0.24	0.26	Bal.

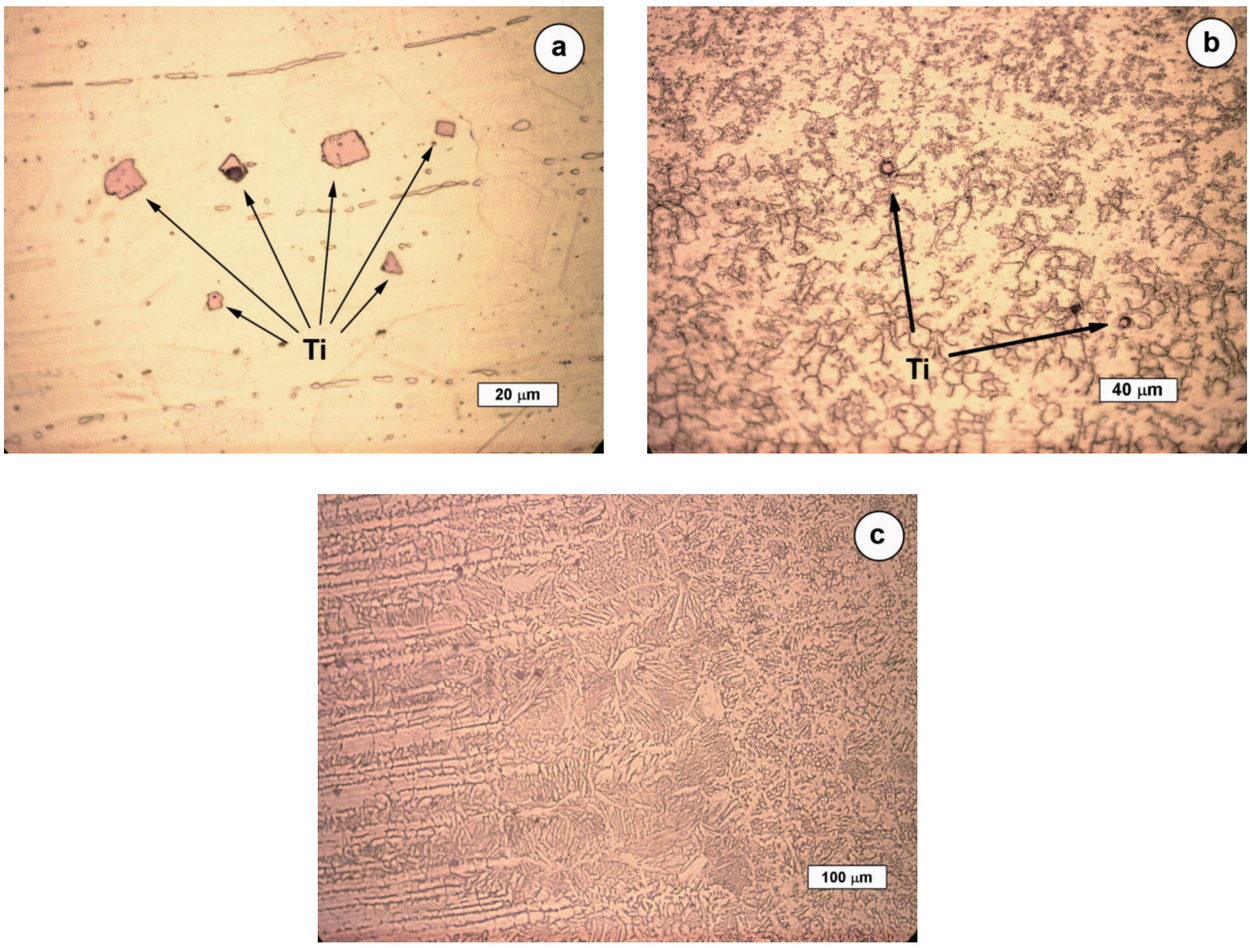

Figure 3. Microstructure of the stainless steel used to manufacture the 250-L water tank; a) Titanium crystals aligned according to lamination bands in the base material; b) Weld metal with titanium crystals visible in its matrix; c) Weld-metal zone close to the base metal showed a Widmanstätten microstructure.

Figura 3. Microestructura del acero inoxidable utilizado en la fabricación del depósito de agua de 250 litros; a) Cristales de titanio alineados en la dirección de las bandas de laminación en el material base; b) Metal de soldadura con cristales de titanio visibles en su matriz; c) En la zona del metal de soldadura próxima al metal base se observa una estructura Widmanstätten.

EDX analyses were carried out by triplicate. These semi - quantitative results correspond with reasonable precision to those expected from the two metals. The Si, Mn, Cr, and Ni contents were similar to obtained by the conventional analysis shown in table II.

In the Ti particles identified in the base metal, there was a high N contribution. This is due to the fact that titanium has a high affinity for nitrogen, which is normally present in stainless steels in amounts of up to 0.05 %. With nitrogen, titanium forms the nitride TiN, and together with carbon the compound titanium carbonitride Ti(CN), whose formation takes place in parallel with that of titanium carbide[12]. The Ti particles found in base metal were typically in the form of TiN because the weight-based ratio of Ti/N is 3.7 versus the weight-based stoichiometric ratio of TiN 3.43. The small difference could have been due to the undetected C content. The amount of Ti retained by N would have been 0.05 × 3.4 = 0.17 %. Since Ti was detected in the base metal in amounts of 0.35 % (Table II), the remaining 0.18 % would have been enough to incorporate all of the stainless steel's C content (0.26 %), thus avoiding HAZ (heat-affected zone) sensitization.

The ferrite in the weld metal was found to have a typical Cr content. The ratio with Nb particles (Nb/Fe) was 0.92 versus a weight-based stoichiometric ratio in the Lewis phase (Fe_2Nb) of 0.83. The 10 % difference was reasonable.

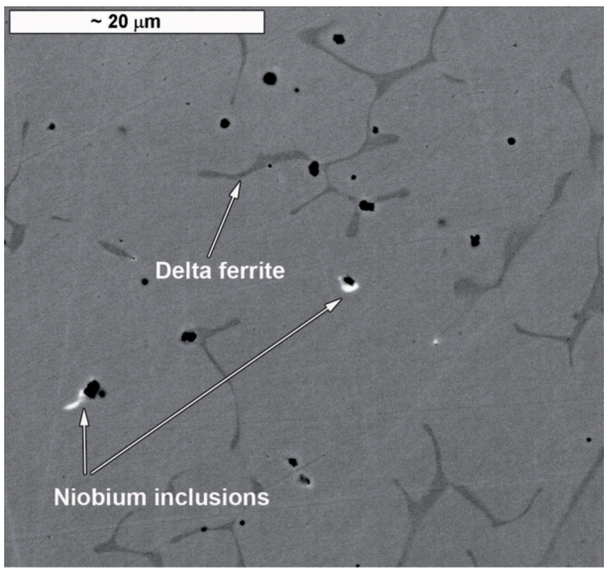

Figure 4. Austenitic matrix containing islands of delta ferrite and niobium inclusions in the weld metal. Image obtained using scanning electron microscopy with back-scattering electron (2,000x).

Figura 4. Matriz austenítica conteniendo islas de ferrita delta e inclusiones de niobio en el metal de aporte. Imagen obtenida utilizando un microscopio electrónico de barrido en modo de electrones retrodispersados (x 2.000).

The Nb content of the weld metal (0.24 %) was not sufficient to compensate for the 0.056 % C content of the weld metal, nor considering a 33 % dilution, a C content of 0.046 %. Since the weld metal additionally contained Ti particles and the ferrite phase had a relatively high chromium content (on the order of 25 wt %), chromium depletion caused by carbon formation was not significant. This explains why, as in this case, weld metal is not generally susceptible to intergranular corrosion[13].

3.2. Corrosion analysis

3.2.1. Corrosion at F-41 weld seam

In the longitudinal weld seam extending from the head to the central circumferential weld seam, unrepaired pitting, denoted as F - 41, was observed and subjected to further analysis. On the outer part of the tank, the water and the corrosion products had obviously drained through the pitting zone and down the tank. The pitting zone was located between the base metal and the weld metal. By partially removing the oxides on the inside, we observed two adjacent pitting zones. Areas in which the pitting had been repaired consistently showed a large agglomeration of micropitting, always located between the base metal and the weld metal and preceding the occurrence of pitting.

For the metallographic study, a series of cuts were made in the original test material to obtain specimens of the appropriate size for study. These were polished and then subjected to electrolytic etching. Optical microscopy showed that pitting had occurred completely within the weld seam, forming a line along the HAZ and barely entering the base metal through the lamination bands (Fig. 5). However, the corrosion then rapidly progressed towards the inside of the weld seam by following its dendritic structure (the interface between delta ferrite and austenite) (Fig. 6).

Table III. Semi-quantitative test, carried out using SEM-EDX, of the different phases observed in the microstructure of the base and weld metals of the 250-L tank under study (n=3) (% in weight)

Tabla III. Análisis semicuantitativo por SEM-EDX de las diferentes fases observadas en la microestructura del material base y del baño de fusión del depósito de 250 litros en estudio (n=3) (% en peso)

Material	Phase	C	Si	Mn	Cr	Ni	N	Ti	Nb	Fe
Base Metal	Matrix	Presence	0.68	1.16	17.98	9.03				69.41
Base Metal	Titanium	Absence			0.77		20.61	76.44		2.16
Weld Metal	Matrix	Presence	0.64	1.34	18.33	9.20				67.04
Weld Metal	Ferrite	Presence	0.70	1.35	23.36	4.79				65.39
Weld Metal	Niobium	Presence	0.65	1.82	13.93	6.39		0.31	33.17	35.96

Figure 5. Pitting corrosion on the base-metal side. The corrosion has progressed along the lamination bands of the base metal.

Figura 5. Corrosión por picaduras en el baño de fusión. La corrosión progresa a lo largo de las bandas de laminación del metal base.

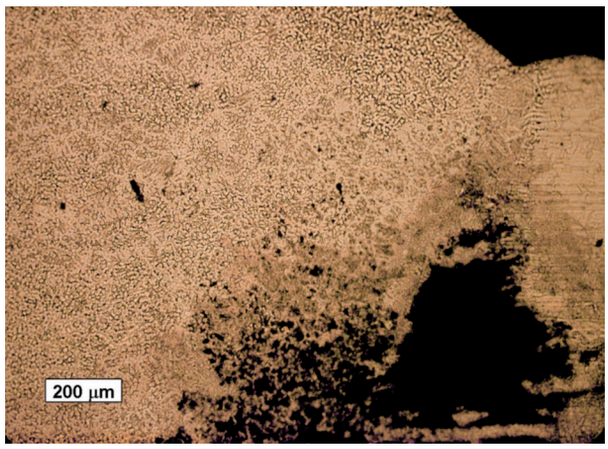

Figure 6. Pitting corrosion on the weld-metal side. The corrosion has progressed along the dendritic phase of the weld.

Figura 6. Corrosión por picaduras en la zona fundida. La corrosión progresa a lo largo de la fase dendrítica de la soldadura.

Corrosion therefore initiated between the base metal and the weld metal, that is, in the HAZ, and progressed rapidly to the welding zone, which acted anodically, but it also involved the base metal, albeit more slowly.

The Ti and Nb used to stabilize austenitic stainless steel protects it against intergranular corrosion, but not against pitting corrosion[12 and 14]. In the aeronautic and aerospace industry at the beginning of the 1940s, and due to the vulnerability of 18-8 stainless steel welds to intergranular corrosion under certain service conditions, Nb was proposed for stabilization purposes. The use of Nb in filler metal was a major advance in the manufacture of this type of stainless steel. Moreover, the addition of Ti improved stainless steel's resistance to intergranular corrosion. The precipitation of titanium carbides reduces the formation of chrome carbides, which occur at low concentrations of Ti. Much more important than the Ti content is a low (0.03 %) C content, which improves resistance to corrosion. Also, the presence of Mo in AISI 316Ti reduces the precipitation of chrome carbides by increasing the stability of titanium carbides and of intermetallic compounds, thus reducing the risk of Cr depletion[15]. Accordingly, the water tanks built in 2007 with AISI 316Ti were only barely corroded.

Among the pitting corrosion products obtained from the F - 41 pit were calcite (80 %), goethite (6.8 %), phyllosilicates (10.3 %), and amorphous compounds (2.9 %). Crystalline forms of sulfur compounds typical of MIC and reflecting the presence of SRB were not found.

3.2.2. Corrosion in the F-11 Nozzle

The interior of the corrosion site F - 11 is shown in figure 7a). F - 11 corresponds to a nozzle made of AISI 316 and was located in the lower zone of the tank. The nozzle was not welded on the inside and none of the welds between the nozzles and the shell plate had been made from the inside. Moreover, most of the nozzles, including the one involving F-11, were blind, with bronze plug pipes.

Observation of the F - 11 nozzle from the inside showed two small pitting on the external zone, where the weld metal and base metal met, which had been repaired. Cutting the nozzle in half revealed that the join between the shell plate and the nozzle had almost completely disappeared due to extensive subsurface pitting. The resulting pits had filled with corrosion products (Fig. 7b) and 7c)).

Electrolytic etching of the polished test specimen showed that in the two pitting zones detected on the inside of the water tank, corrosion ran along the edge of the welding, progressing toward the interior but hardly towards the tank's base metal (Fig. 7c)). In no case did the corrosion involve nozzle material made of AISI 316. As noted above, this was due to the fact that AISI 316 contains Mo, which makes it resistant to pitting corrosion. The influence of alloyed Mo in

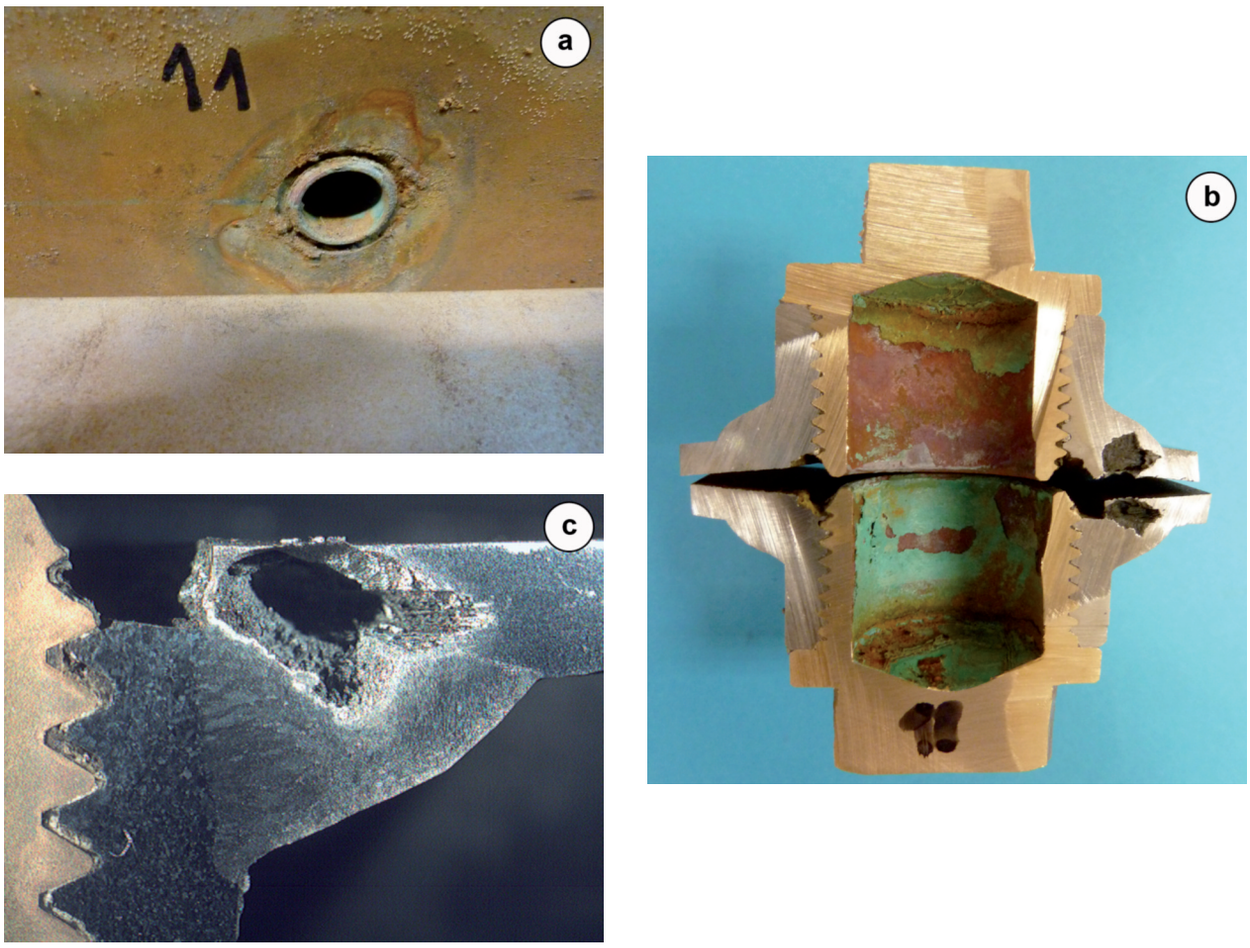

Figure 7. a) Interior of the F-11 specimen obtained from the 250-L water tank, corresponding to a nozzle welded only on the outside and fitted with a bronze plug pipe; b) Nozzle cut in two sections; c) Enlargement of b), showing subsurface pitting almost completely occupying the weld section.

Figura 7. a) Interior de la probeta F-11 obtenida del depósito de agua de 250 litros, correspondiente a la tubuladura soldada solamente por el exterior con una tubería de bronce; b) Tubuladura cortada en dos secciones; c) Detalle de b), demostrando la picadura subsuperficial que ocupa prácticamente toda la sección de la soldadura.

increasing the pitting resistance of stainless steels is well documented in the literature for many years[16 and 17 and references therein]. The different stages of pitting are nucleation, initiation, propagation or repassivation of pits. Alloyed Mo doesn't show a strong action on the surface of the passive metal and consequently in the nucleation and initiation stages. During the initiation stage dissolution kinetics are crucial in the production of active molybdenum species. Alloyed Mo is efficient in retarding the propagation of metastable pits because can slow down the kinetics of pit growth in processes taking place inside the pits, such as pit growth or repassivation. Increasing Mo content repassivation take place earlier[18].

3.2.3. *Tank-water analysis*

Physicochemical analysis of the tank water showed a significant concentration of chlorides, up to 175 ppm (Table IV). The water in the trains' tanks comes from the storage facility at Can Tunis (Barcelona, Spain), which is located close to the sea.

The bacteriological test results are also shown in table IV. The total number of aerobic bacteria was much higher than that recommended for drinking water (<100 CFU/100 ml). However, this aerobic load was not accompanied by anaerobic contamination by SRB, which were not detected after 21 days of incubation.

Table IV. Characteristics of the water found in the hotel trains

Tabla IV. Características del agua encontrada en los trenes hotel

Parameter	Hotel Train 7C9	Hotel Train 7C8
Chloride (ppm)	148.00	175.80
Sulfate (ppm)	90.49	127.50
Nitrate (ppm)	0.00	9.10
Fluoride (ppm)	1.10	0.00
Carbonate (ppm)	0.00	0.00
Bicarbonate (ppm)	161.59	192.07
Sodium (ppm)	87.90	89.00
Potassium (ppm)	21.20	13.30
Calcium (ppm)	69.80	96.90
Magnesium (ppm)	15.00	19.70
pH	7.31	8.16
Conductivity (μS/cm)	1,060	1,140
Total aerobic bacteria (CFU/100 ml)	N.D.	4.36×10^6
Sulfate-reducing bacteria (SRB)	N.D.	Negative

N.D. = Not determined.

In general, chlorides are detrimental to stainless steel, especially austenitic stainless steel, in which they cause pitting corrosion. Protection against pitting in austenitic stainless steel is basically carried out by adding Mo, which was present in AISI 316 but practically absent in AISI 321. The addition of Mo has been shown to confer pitting resistance to dilute chloride solutions[6]. However the maximum concentration of chloride permissible for these types of stainless steel is 100 ppm[13 and 16].

4. CONCLUSIONS AND GUIDELINES

— The water tanks were correctly manufactured and complied with the specifications of the manufacturing procedures. The quality of the material was appropriate and there were no defects in the welding. MIC due to the presence of anaerobic SRB could be ruled out because: 1) the morphology of the pitting was not characteristic of this type of corrosion; 2) neither SRB nor their typical sulfide-based metabolites were found in the corrosion products; 3) SRB were not detected in the tank water. It was thus concluded that the pitting corrosion problems were due to an incompatibility between the tank-construction materials and the quality of the water contained in the tanks. Accordingly, the following recommendations address both the tank materials and the quality of the tank water.

— About austenitic stainless steel.
Of the materials used in the construction of the water tanks, the best qualities were obtained with AISI 316Ti welded with Mo-containing ER-316L. The presence of Mo confers protection against pitting corrosion.
AISI 321 stainless steel welded with ER347, while less expensive than AISI 316Ti, is inadequate as it is vulnerable to pitting corrosion.
An alternative to AISI 316Ti is a non-stabilized stainless steel such as AISI 316. If, for reasons of design, a thicker tank is required, AISI 316 could be used if the C content were restricted to a maximum of 0.03 %. The filler metal would then have to be ER-316L, with measures taken to minimize heat input during welding.

— About the tank water.
Tank water should be analyzed for the presence of materials that aggressively interact with the tanks, especially if they are constructed from materials not resistant to pitting corrosion. Should not be allowed the AISI 321 to come in contact with tank water containing chlorides in concentrations > 100 ppm. Therefore, in the case analyzed in this study, the quality of the water used to fill the tanks should be improved.

Additional recommendations

For water tanks currently in use, we recommend magnesium anodes to protect the inside of the tanks.

In the future, tank design can be improved by minimizing the immersion welds, moving some of them to the upper zone, and by eliminating unnecessary nozzles. An increase in the diameter of the nozzles would allow the addition of sacrificial anodes in the form of bars.

REFERENCES

[1] J.R. Ibars, D.A. Moreno and C. Ranninger, *Microbiologia SEM* 8 (1992) 63 - 75.

[2] J.R. Ibars, D.A. Moreno and C. Ranninger, *Int. Biodeter. Biodegr.* 29 (1992) 343 - 355.

[3] M. Bibb, Bacterial Corrosion in the South African Power Industry, in *Biologically Induced Corrosion*, S.C. Dexter (Ed.), NACE, Houston, Texas, USA, 1986, pp. 96 - 101.

[4] D.H. Pope, D.M. Dziewulski and J.F. Kramer, *1988, Workshop Proceedings*, George Licina (Ed.), EPRI, Palo Alto, USA, 1989, pp. 3 -1/3 - 24.

[5] S.W. Borenstein, *Mater. Performance* 30 (1991) 52 - 54.

[6] ASM Handbook, Vol. 6: *Welding, Brazing and Soldering*. 9th edition, ASM International (1993).

[7] ASTM A262: Standard Practices for Detecting Susceptibility to Intergranular Attack in Austenitic Stainless Steels, *Book of Standards*, Vol. 01.03, ASTM International, Philadelphia, USA, 2008.

[8] J.R. Postgate, *The Sulphate-Reducing Bacteria*, 2nd edition, Cambridge University Press, 1984.

[9] APHA, AWWA, WEF: *Standard Methods for the Examination of Water and Wastewater: Centennial Edition*, 21st edition. A.D. Eaton, L.S. Clesceri, E.W Rice, A.E. Greenberg, M.A.H. Franson (Eds.), Washington, DC, USA, 2005.

[10] S.A. David, J.M. Vitek, R.W. Red and T.L. Hebble, Effect of Rapid Solidification on Stainless Steel Weld Metal Microstructures and Its Implications on the Schaeffler Diagram, Oak Ridge National Laboratory, TM – 10487, Tennesse, USA, 1987.

[11] S.A. David, *Weld. J.* 60 : 4 (1981) s63 - s71.

[12] E. Folkhard, G. Rabensteiner, E. Perteneder, H. Schabereiter and J. Tösch, *Welding Metallurgy of Stainless Steel*, Springer-Verlag 1988.

[13] ASM Handbook, Vol. 13. *Corrosion*, 9th edition, ASM International, 1987.

[14] *Welding Handbook*, Vol. 4: *Materials and Applications*, *Part 2*, 8th edition, American Welding Society, Miami, Florida, USA, 1998.

[15] A. Pardo, M.C. Merino, A.E. Coy, F. Viejo, M. Carboneras and R. Arrabal, *Acta Mater.* 55 (2007) 2239 - 2251.

[16] Z. Szklarska-Smialowska, *Pitting Corrosion of Metals*, NACE, Houston, Texas, USA, 1986.

[17] A.J. Sedriks, *Corrosion of Stainless Steels*, Ed. John Wiley & Sons, Inc., 1979.

[18] S. Virtanen and W. Tobler. *Electrochemical Society Proceedings*, P. Schmuki, D.J. Lockwood, Y.H. Ogata, M. Seo and H S. Issacs (Eds.) 2004, pp. 265 - 271.